Clinical Ophthalmology

Dovepress
open access to scientific and medical research

Open Access Full Text Article

REVIEW

Clinical applications of optical coherence tomography in the posterior pole: the 2011 José Manuel Espino Lecture - Part I

This article was published in the following Dove Press journal:
Clinical Ophthalmology
7 November 2013
Number of times this article has been viewed

J Fernando Arevalo[1,2]
Andres F Lasave[3]
Juan D Arias[3]
Martin A Serrano[3]
Fernando A Arevalo[3]

[1]Retina Division, Wilmer Eye Institute, Johns Hopkins University School of Medicine, Baltimore, MD, USA; [2]Vitreoretinal Division, King Khaled Eye Specialist Hospital, Riyadh, Kingdom of Saudi Arabia; [3]Retina and Vitreous Service, Clinica Oftalmologica Centro Caracas, Caracas, Venezuela

Abstract: Optical coherence tomography (OCT) is now a standard of care in ophthalmology and is considered essential for the diagnosis and monitoring of many retinal diseases. One of the major advances obtained with OCT was the understanding of the pathophysiology of macular holes. Non-full-thickness macular holes have been revisited because high-resolution OCT images can detect a lamellar macular defect that is not always visible clinically, and surgery has been advocated by some authors. OCT can be valuable in determining the need for and/or timing of surgical intervention on epiretinal membranes or vitreomacular traction syndrome. In addition, we can use this technology as a predictive factor in the prognosis and follow-up of the most common posterior pole pathologies.

Keywords: clinical applications, OCT, optical coherence tomography, posterior pole, retinal diseases, spectral domain

Introduction

Optical coherence tomography (OCT) is a very useful imaging technology in general medicine because it performs a real-time "optical biopsy."[1,2] Therefore, this diagnostic tool allows the identification of morphologic details that previously could be visualized only through histopathologic analysis. In ophthalmology, OCT has become an essential tool because it can identify early stages of disease before symptoms and irreversible vision loss occurs. OCT is a rapid, noncontact, and noninvasive examination method of imaging intraocular tissue that has significantly improved the potential for early diagnosis, understanding of retinal disease pathogenesis, and monitoring of disease progression and response to therapy.

In recent years, OCT techniques have evolved from the initial time-domain OCT method with an axial resolution of 15 μm and a scanning speed of 400 A scans per second to spectral domain OCT (SD-OCT), which features a higher speed and improved resolution, presenting an axial resolution of 5 μm and a scanning speed of up to 50,000 A scans per second in commercially available systems. Most importantly, these advanced OCT systems are based on a raster scanning method and provide a three-dimensional (3D) reconstruction of the entire macular region.[3–5]

Until the advent of OCT, available techniques for ocular imaging did not have sufficient depth resolution in the posterior segment of the eye to provide useful cross-sectional images of retinal structure.[6–8] This imaging technology was demonstrated in 1991 by Huang et al.[6] OCT has had the most clinical impact in ophthalmology, where it provides structural and quantitative information that cannot be obtained by any other modality. The development of OCT in ophthalmology proceeded rapidly. The

Correspondence: J Fernando Arevalo
Vitreoretinal Division, The King Khaled Eye Specialist Hospital, Al-Oruba Street, PO Box 7191, Riyadh 11462, Kingdom of Saudi Arabia
Tel +966 1 482 1234 ext 3860
Fax +966 1 482 1234 ext 3727
Email arevalojf@jhmi.edu

submit your manuscript | www.dovepress.com
Dovepress
http://dx.doi.org/10.2147/OPTH.S51098

first in vivo retinal images were obtained independently in 1993 by Fercher et al[8] and Swanson et al,[9] and the first commercial device for use in posterior segment structures became available in 1995 (OCT 1; Humphrey Instruments, Dublin, CA, USA). The technology was transferred to industry and introduced commercially for ophthalmic diagnostics in 1996 (Carl Zeiss Meditec, Jena, Germany). A third-generation ophthalmic instrument (Stratus OCT; Carl Zeiss Meditec) was introduced in 2001. To improve image resolution and scanning speed, a high-definition and SD-OCT system (Cirrus, Carl Zeiss Meditec) was developed in 2006, and it is now a natural successor of Stratus OCT, allowing for even higher resolution at simultaneously increased scanning speed. Today, there are several options on the market for SD-OCT.

With an axial resolution of between 5 μm and 10 μm, according to the equipment used, SD-OCT provides the best visualization of retinal architecture of any imaging technique currently available.[6,10] The unprecedented speed and resolution of OCT technology has allowed ultramicroscopic structural evaluation of the posterior pole of the eye at an extremely fine spatial scale. Currently in retinal diagnosis, decisions for surgical interventions are based to a high degree on this imaging technology. In addition, as an OCT examination is standardized and easy to perform, it can easily be delegated to specially trained technicians and introduced as a routine procedure. Consequently, the increased use of OCT has dramatically affected diagnostic and therapeutic approaches in recent years.[11–13] OCT is now a standard of care in ophthalmology and is considered essential in the diagnosis and monitoring of many retinal diseases; it is also a useful tool when making decisions regarding surgical intervention.

The objective of this article is to review the basic principles, interpretation, and clinical applications of OCT in vitreoretinal interface disorders of the posterior pole.

Basic principles

OCT imaging is analogous to ultrasound imaging, except that it uses infrared light reflections rather than acoustic waves. Cross-sectional images are generated by scanning an optical beam across the tissue and measuring the echo time delay and intensity of backscattered light. OCT is based on an optical measurement technique known as low coherence interferometry, which can be used to measure distances to objects (ocular structures) with high precision by measuring the light reflected from them. The low coherence light used is produced by a superluminescent diode that is directly coupled into an optical fiber of Michelson's interferometer. The fiber-optic implementation provides a compact and robust system that can be interfaced to a variety of clinical imaging instruments. Two hundred microwatts of infrared light at 820 nm are emitted on the retina, which is consistent with the American National Standards Institute Classification System,[14] for intrabeam viewing. The interferometer divides the light source into a measurement light path and a reference light path. The light beam is launched into the eye, and backscattered or backreflected light gives information about the distance and thickness of the different retinal microstructures.

The coherence length of the light source determines the axial resolution of the OCT; systems used in experimental research can achieve resolutions from 10–15 μm to 1–5 μm.[15] Ultrahigh resolutions of 3 μm have been achieved in ophthalmic imaging, enabling visualization of internal retinal architectural morphology and promising to improve the accuracy and reproducibility of retinal morphometry.[16,17]

A high-power objective lens (+78 diopters) is used so that the retina is imaged onto an image plane inside the instrument. OCT bidimensional B-scan images are constructed by performing rapid, successive axial measurements at different transverse points similar to B-scan ultrasound imaging. The conventional time domain (Stratus OCT) has an axial scan repetition rate of approximately 400 (128 to 768) axial scans per 2.5 seconds (1 second in the commercial unit). SD-OCT technology provides an axial resolution of 5 μm and a scanning speed of up to 50,000 A-scans per second. Others advantages of SD-OCT are improved image quality, improved coverage of the retina, registration of OCT findings to fundus features, longitudinal tracking of pathology, and 3-D imaging.

OCT is well tolerated because it is a noninvasive procedure, and images can be acquired rapidly without eye contact and at low light intensity. The position of each scan is registered by the computer to allow future OCT examinations to be performed on the same exact location. The final OCT image is displayed using a false color map that corresponds to detected backscattered light levels from the incident light. The high reflectivity signals are represented by white and red colors, while the low reflectivity signals are represented by black and blue colors. The scattering from cataracts, vitreous hemorrhage, and corneal edema produce a reduction in image intensity; however, it does not degrade image quality except in cases of severe opacity.

Ophthalmic applications in the posterior pole

OCT is especially convenient in ophthalmology, due to the optic eye properties and easy accessibility of the retina for the exam. The OCT system hardware consists of the patient

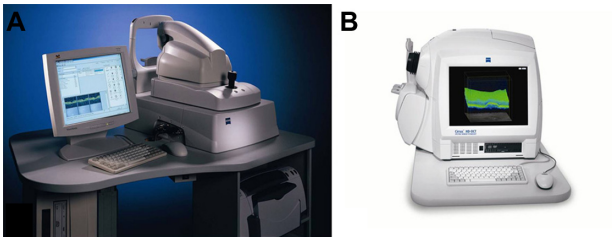

Figure 1 OCT device.
Notes: (**A**) Stratus OCT 3000. (**B**) High-resolution Cirrus (both courtesy of Carl Zeiss Meditec, Jena, Germany).
Abbreviation: OCT, optical coherence tomography.

module and the computer unit (Figure 1). The patient module sends the OCT scan to the retinal area of interest, and the video monitor receives and analyzes the OCT image. OCT has characterized a wide variety of retinal diseases, and the OCT images correspond with the retinal morphology of these illnesses viewed by light microscopy.[18,19] OCT provides a powerful adjunct to conventional fundus and fluorescein angiography that can function not only as a sensitive disease diagnostic test, but also can be used to track disease progression and monitor treatment.

Interpretation

OCT is an imaging method for high resolution, cross-sectional visualization of tissue. Therefore, OCT interpretation requires appropriate knowledge of the normal anatomy of the eye fundus. OCT allows carrying out an "optic biopsy" because it delineates the layers of the retina (Figure 2).

A highly scattering layer (70 µm in thickness), which is visible as red, delineates the posterior boundary of the retina in the tomogram and corresponds to the retinal pigment epithelium (RPE) and choriocapillaris complex.[10] The nerve fiber layer appears as a highly backscattering red layer at the vitreoretinal interface. The RPE and nerve fiber layer define the posterior and anterior boundaries of the sensory retina, respectively; these boundaries are important in quantifying neurosensorial retinal thickness on OCT.[20] Retinal areas of relative low reflection correspond to the location of the nuclear layers. The vitreoretinal interface can be seen in OCT images as a high-contrast boundary between the vitreous and retina. The normal vitreous gel is optically transparent, and therefore not visible in OCT imaging. The choroid and RPE together match to a wide band of retinal high reflection that decreases at greater choroidal and scleral depth.

OCT images demonstrate reproducible patterns of retinal morphology that correspond to the location of retinal layers seen on light microscopy.[21] Layers of relative high reflectivity

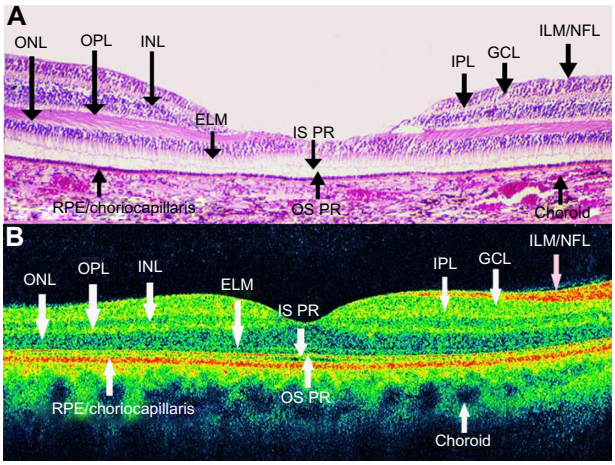

Figure 2 OCT shows a normal eye.
Notes: It has been considered that OCT allows carrying out of an "optic biopsy" because it delineates the layers of the retina. (**A**) Pathological anatomy of the fovea. (**B**) OCT of normal macula with different layers of the retina labeled (IS PR; now known as Ellipsoid Zone on the OCT image).
Abbreviations: ELM, external limiting membrane; GCL, ganglion cell layer; ILM/NFL, internal limiting membrane/nerve fiber layer; INL, inner nuclear layer; IPL, inner plexiform layer; OPL, outer plexiform layer of Henle; IS PR, inner segments of photoreceptors (hyoid and ellipsoid segments); OCT, optical coherence tomography; ONL, outer nuclear layer; OS PR, photoreceptor's outer segments; RPE/choriocapillaris, retinal pigment epithelium and choriocapillaris complex.

correspond to horizontally aligned retinal components such as the nerve fiber layer and plexiform layers as well as to the RPE and choroid. In contrast, the nuclear layers demonstrate relative low reflectivity. In the fovea, there is a convergence of relative low reflection layers, with only a single outer band of relative low reflection present in the center of the fovea (Figure 3).

Foveal thickness has been calculated to be 147 ± 17 µm in normal eyes with time-domain OCT.[22] However, Han and Jaffe[23] compared retinal thickness measurements obtained by SD-OCT and time-domain OCT in eyes with and without posterior segment disease diagnoses. They obtained a foveal thickness of

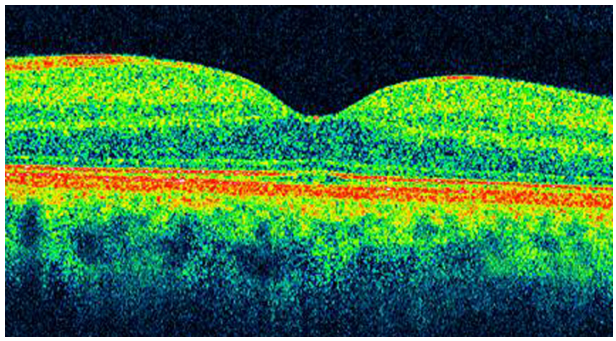

Figure 3 Optical coherence tomography image shows a normal foveal contour.
Notes: Axial section showing the external limiting membrane, the inner segment/outer segment junction (Ellipsoid Zone), the retinal pigment epithelium, and the choroid. Observe that the foveal contour is at exactly the same level of the outer plexiform layer.

206 ± 25 µm, 259 ± 19 µm, and 279 ± 21 µm in normal eyes with Stratus OCT, Cirrus SD-OCT, and Spectralis (Heidelberg Engineering, Heidelberg, Germany) OCT, respectively.

The discrepancy among the three devices in terms of macular thickness values reflects differences in defining retinal segmentation algorithms. While Stratus OCT measures the thickness of the retina as the distance between the inner limiting membrane (ILM) and the junction of the outer segment and inner segment of the photoreceptors, Cirrus SD-OCT reports it as the distance from the anterior border of the retinal pigment epithelium to the ILM[24] and Spectralis OCT measures the distance from the posterior border of the RPE to the ILM. Therefore, the macular measurements are larger on Spectralis OCT compared to Cirrus SD-OCT and Stratus OCT. The mean difference between macular thickness measurements obtained by the Cirrus SD OCT and Stratus OCT in nine different subfields was close to 50 µm in most of the subfields, which is the length of the outer segment of human photoreceptors.[24,25]

Clinical applications of OCT in the posterior pole

Vitreoretinal interface disorders

Macular hole

Idiopathic macular hole is a retinal disease characterized by a full-thickness defect of the foveal area with associated visual acuity reduction, metamorphopsia, and a central scotoma. OCT has improved the understanding and management of idiopathic macular hole. Its incidence is around three in 1,000, and it is more common in females between 50 and 60 years of age.[26] The pathophysiology of the development of idiopathic macular hole has been extensively studied.[27–29] In the 1970s, recent posterior vitreous detachment was usually noted in eyes with macular holes, while eyes with pre-existing vitreous detachment very rarely developed a macular hole. This observation led to the conclusion that vitreous traction plays an important role in macular hole formation.[30] In 1983, Avila et al suggested that the main cause of macular hole formation was anteroposterior traction exerted by vitreous fibers on the center of the fovea.[31] In 1988, Gass[27] introduced the concept of tangential traction of the vitreous cortex at the foveolar edges as the etiology of macular holes. Immediately, foveal dehiscence was followed by centripetal retraction of retinal elements.[27] The posterior hyaloid face of the vitreous remained attached to the foveola and surrounding macular region at the initial stages of hole formation.[32] In 1995, the same author suggested that most full-thickness macular holes arise from an umbo dehiscence without loss of foveal tissue.[33]

Although slit lamp observations and photographic documentation were provided, adequate imaging of the posterior hyaloid detachment and retinal layers was impossible before the OCT era. With the help of the OCT, other investigators have proposed that the hole formation involves vitreoretinal separation with vitreofoveal adhesion exerting oblique traction on the fovea, followed by foveal cysts or foveal detachment, foveal dehiscence, and finally full-thickness hole formation.[27,28]

OCT staging with some modification can parallel the staging of macular holes with biomicroscopic examination. OCT has demonstrated changes in the vitreomacular interface not visible with biomicroscopy (Figure 4). It is now widely accepted that the early event leading to macular holes is the persistent adherence of the cortical vitreous to the fovea with adjacent vitreoretinal separation. The resultant traction on the fovea causes foveal detachment or an intraretinal space, termed pseudocyst. Further traction leads to dehiscence of foveal tissue, resulting in full-thickness macular hole formation.[34,35]

Classification of idiopathic macular holes as proposed by Gass[27,29] has always been the standard in staging macular holes. However, sometimes the determination of the developmental stage of macular holes was difficult to assess clinically. Since the introduction of the OCT, staging of macular holes has changed, especially with respect to the early stages.

Gass classification[27,29] indicates that Stage 1 holes (foveal detachment) may be distinguished by a reduced or absent foveal pit and the presence of an optically clear space beneath the fovea, suggesting a foveolar detachment. There is vitreomacular traction due to posterior incomplete vitreous detachment lifting the foveal area and the formation of an impending macular hole. This clinically appears as a yellowish spot on the fovea. Depending on how soon the patient is examined after the onset of symptoms and the degree of elevation of the retina, either a yellow spot

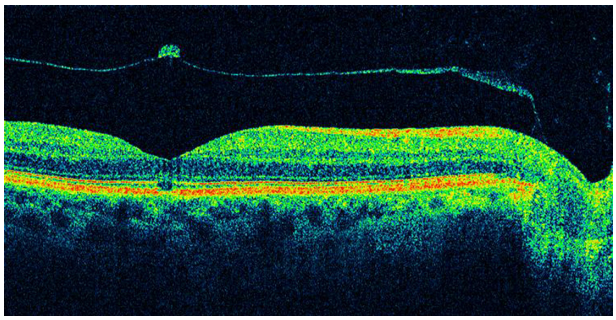

Figure 4 Optical coherence tomography has demonstrated changes in the vitreomacular interface not visible with biomicroscopy.

100–200 µm in diameter (Stage 1A) or a yellow ring approximately 200–350 µm in diameter (Stage 1B) is present in the foveolar area. As the foveolar retinal detachment (Stage 1A) progresses to foveal retinal detachment (Stage 1B), the progressive stretching and thinning of the foveolar center may cause the redistribution of the xanthophyll pigment into a ring configuration.

Stage 2 holes are those in the early hole formation stage. In the majority of patients, the yellow ring enlarges and a full-thickness retinal dehiscence will develop within several weeks or months. This stage shows a partial break on the surface of the retina while the operculum is still attached to the retina, or separated from the underlying retina with a small full-thickness loss of retinal tissue of less than 400 µm in size.

Stage 3 holes have a full-thickness retinal dehiscence with a complete break in the outer retinal tissue, and variable amounts of surrounding macular edema that increase retinal thickness and decrease reflectivity in the outer retinal layers. In this stage, there is complete separation of the operculum from the underlying retina, with a hole diameter greater than 400 µm.

Stage 4 holes may be characterized by the complete loss of tissue greater than 400 µm in size and a complete posterior vitreous detachment with release of the anteroposterior tractional forces.

Stage 1 and 2 macular holes are very difficult to differentiate ophthalmoscopically, and high-resolution OCT images can help to classify them, Stage 2 often progresses to Stage 3 with some visual loss; appropriate staging with OCT can help to determine when surgery is indicated.[36]

Vitreoretinal traction is very important in the pathogenesis of macular holes, and it can be identified by OCT.[37] Duker et al[38] found vitreoretinal interface abnormalities with OCT in 21% of fellow eyes. Furthermore, OCT may be a useful method of assessing the risk for hole formation in the fellow eye of patients with a unilateral macular hole. Considering that the probability of developing a macular hole in the contralateral eye is 13% in 48 months,[39] it is then mandatory to perform bilateral tomographic imaging in patients affected by this pathology for early detection in the other eye. However, surgery in the normal contralateral eye of patients with macular holes is not acceptable.

OCT is effective in staging macular holes, and quantitative information may be directly extracted from the OCT tomograms, including the status of the vitreoretinal interface, the diameter of the hole, and the extent of surrounding subretinal fluid accumulation.[4,37] OCT is useful in differentiating simulating lesions and in allowing better counseling of patients regarding their disorder.

In addition, accurate assessment of macular hole size is important for both research studies and to guide clinical management. The size of a macular hole has been shown to affect anatomical and visual success. Macular hole size and postoperative resolution can be evaluated by OCT.[40–42]

Altaweel et al[40] published the latest staging of idiopathic macular holes based on OCT findings. In Stage 1A, OCT demonstrates perifoveal posterior vitreous detachment with continued foveolar adherence. Tractional forces are anteroposterior and tangential. Retinal tissue remains at the base of the pseudocyst. Pseudocysts form (hyporeflective image on OCT) without affecting all retinal layers and with an intact outer retina. In Stage 1B, the foveal pseudocyst affects all retinal layers, including the photoreceptor layer, with an intact roof. There is incomplete posterior vitreous detachment with persistent adhesion onto the fovea in Stages 1A and B (Figure 5). In Stage 2A, the roof of the pseudocyst has been torn open and continues to have traction exerted by the vitreous attachment. There is persistent traction of the posterior hyaloid that is firmly attached to the inner retina. The break in the roof of the pseudocyst gives rise to a full-thickness macular hole. In Stage 2B, the roof of the pseudocyst has completely separated from the retina. At this point, there is release of the anteroposterior tractional forces. The distance between the edges of the hole is less than 400 µm. In Stage 3, the prefoveal operculum can still be appreciated, but the distance between the hole edges is greater than 400 µm. The posterior hyaloid is completely

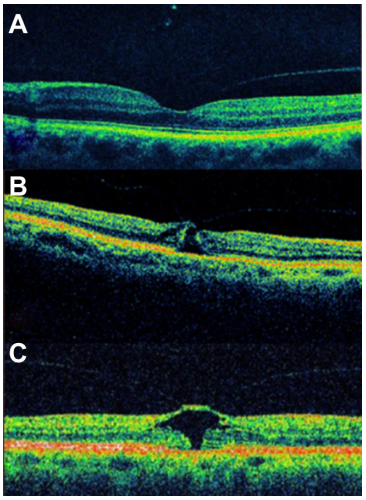

Figure 5 Full-thickness macular hole classification.
Notes: (**A**) Stage 0: Preimpending hole. (**B**) Stage 1A: OCT demonstrates perifoveal posterior vitreous detachment with continued foveolar adherence. Tractional forces are anteroposterior and tangential. Retinal tissue remains at the base of the pseudocyst. (**C**) Stage 1B: In this stage, the pseudocyst enlarges and extends to the retinal pigment epithelium. Foveolar detachment (impending hole) is present.
Abbreviation: OCT, optical coherence tomography.

detached from the inner retina, as opposed to the description by Gass[27] wherein the former remains attached to the perifoveal area. In Stage 4, there exists complete vitreous detachment which cannot be seen tomographically and can only be confirmed by slit lamp biomicroscopy or ultrasonography (Figures 6–9).

The main differences between the biomicroscopic and the OCT staging of idiopathic macular holes are: the presence of a tight focal foveolar adherence of the posterior hyaloid versus a perifoveal vitreomacular detachment; the formation of a foveal pseudocyst versus a detachment in Gass' Stage 1 hole; and the subdivision of Stage 2 into two distinct anatomical types (Table 1).

In those cases with a base diameter less than 400 μm as measured by OCT, an anatomic closure was achieved in 92%; in those with a base diameter more than 400 μm, this value decreased to 56%.[19] Variables such as preoperative visual acuity, symptoms duration, hole diameter by OCT (as a single variable), and stereoscopic fundoscopy may predict the final visual outcome.[41,42] One study demonstrated that OCT measurement is not only predictive of the possibility for anatomic closure but also of postoperative visual acuity outcome. By using the maximum hole diameter, minimum hole diameter, and height as reference values, the authors use a formula to infer macular hole prognosis.[42]

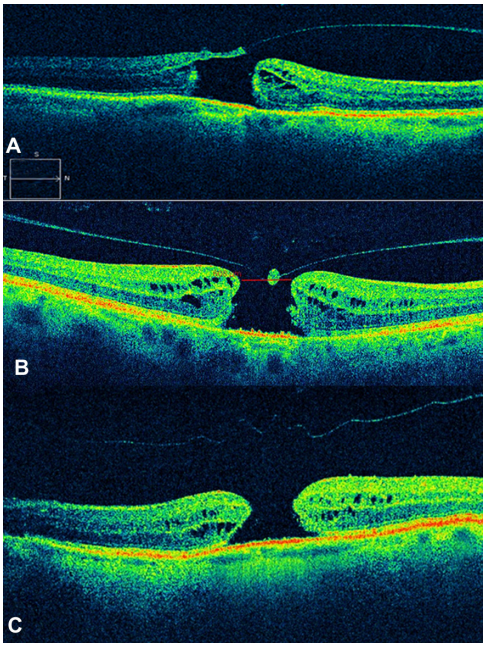

Figure 6 Full-thickness macular hole classification.
Notes: (**A**) Stage 2A. The roof of the pseudocyst has been torn open and continues to have traction exerted by the vitreous attachment. (**B**) Stage 3. Image shows a full-thickness retinal dehiscence with a complete break in the outer retinal tissue. There is complete separation of the operculum from the underlying retina, with a hole diameter of more than 400 μm. Full-thickness macular hole (>400 μm). (**C**) Stage 4. A complete loss of tissue more than 400 μm in size is seen with a complete detachment of the posterior vitreous and release of the anteroposterior tractional forces. Full-thickness macular hole plus complete vitreous detachment.

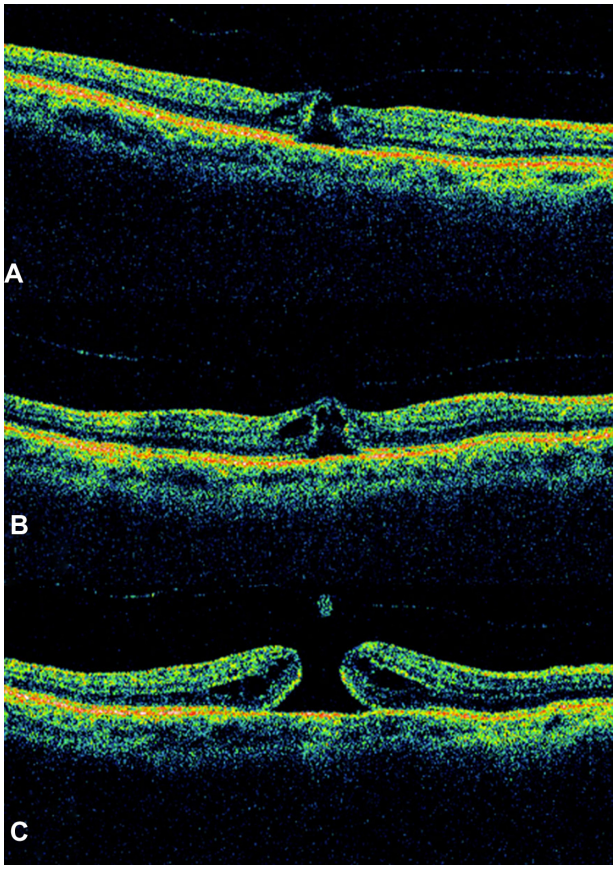

Figure 7 Sequential foveal tomographic images by time-domain optical coherence tomography.
Notes: (**A**) At the initial visit, small intrafoveal splits are seen between the inner and outer retina of a typical Stage 1A macular hole, with the posterior hyaloid reflecting a perifoveal posterior vitreous detachment with continued foveolar adherence that progresses to Stage 1B at 1 month follow-up (**B**). (**C**) After intravitreal injection of tissue plasminogen activator, a full-thickness macular hole was presented.

OCT is likewise useful in evaluating anatomic closure after macular hole surgery (Figure 10). The flattening of the retina and the disappearance of the retinal cysts may be appreciated postoperatively. The closure of the horizontal component of a hole wherein there is complete detachment usually takes place in the first postoperative days. Absence of closure within the first postoperative month entails poor

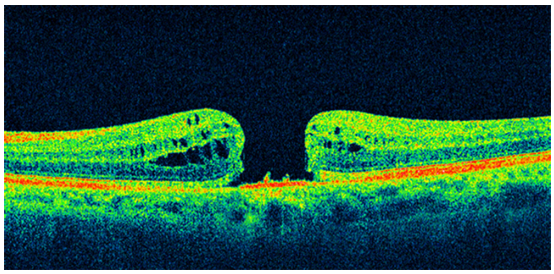

Figure 8 Optical coherence tomography image showed a full-thickness macular hole with complete vitreous detachment.

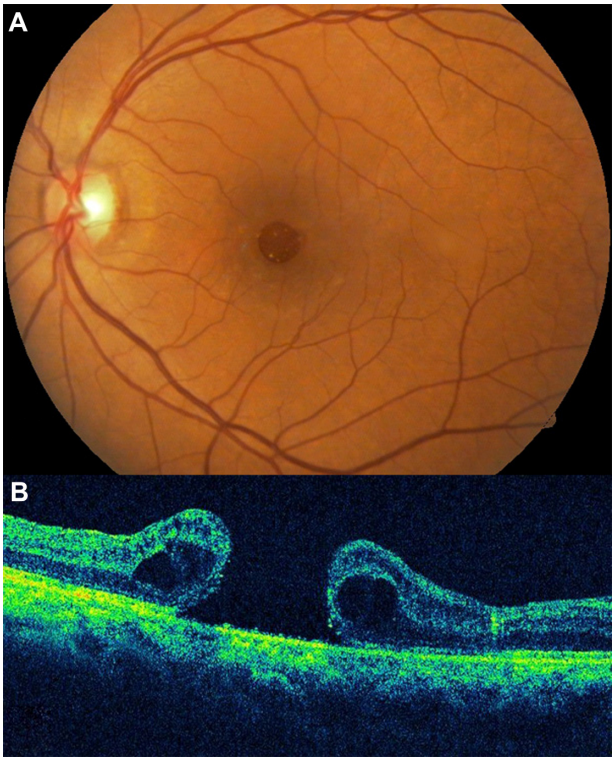

Figure 9 A case of a Stage 4 macular hole.
Notes: (**A**) Color picture of a full-thickness macular lesion. (**B**) Optical coherence tomography image demonstrates a surrounding macular edema that increases retinal thickness and decreases reflectivity in the outer retinal layers. A full-thickness macular hole and complete vitreous detachment is observed.

Table 1 Main differences between the biomicroscopic and the OCT staging of idiopathic macular holes

Biomicroscopic staging[29]	OCT staging[40]
Stage 1A: Foveal dehiscence, yellow spot, posterior hyaloid attached to ILM	Stage 1A: Partial thickness pseudocyst with perifoveal posterior vitreous detachment
Stage 1B: Lateral spread of retinal receptors	Stage 1B: Full-thickness pseudocyst with roof
Stage 2: Full-thickness macular hole, can opener tear or pseudo-operculum, <400 μm diameter	Stage 2A: Partial opening of roof, focal vitreous attachment to flap
Stage 3: ≥400 μm diameter, pseudo-operculum	Stage 2B: Operculated, traction to retina released
Stage 4: Complete PVD	Stage 3: ≥400 μm diameter, operculated, traction released
	Stage 4: Complete PVD, vitreous face not evident on OCT

Abbreviations: ILM, internal limiting membrane; OCT, optical coherence tomography; PVD, posterior vitreous detachment.

prognosis.[33] In the normal course of an idiopathic macular hole, about 2% may close by itself spontaneously when there is release of vitreomacular traction. In such cases, the photoreceptors may be affected due to the previously existing traction, and as a result may give rise to an absolute central scotoma.

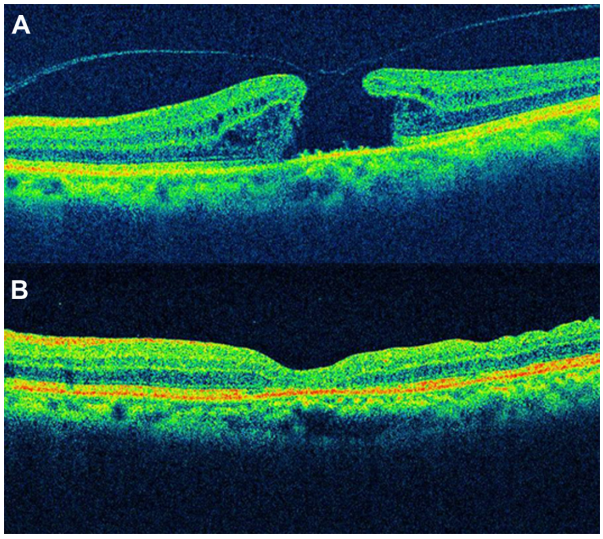

Figure 10 Spectral domain optical coherence tomographic images of a 68-year-old patient with a full-thickness macular hole.
Notes: (**A**) Before surgery; (**B**) 6 months after surgery, good foveal contour was achieved and the visual acuity improved from 20/200 to 20/80.

Non-full-thickness macular holes

The description and pathogenesis of non-full-thickness macular holes have been better understood with the advent of OCT. Lamellar macular hole (LMH) and macular pseudohole can be a different clinical manifestation of the same disease.

LMH was first described by Gass[43] in 1975 as an abortive process of full-thickness macular hole formation resulting from deroofing of cystoid macular edema. Instead, macular pseudohole was described as being caused by centripetal contraction of previously present epiretinal membrane, which surrounds but does not cover the foveal area.[44] However, it is possible that the coexistence and possible evolution from a macular pseudohole to lamellar macular hole follows progressive ERM contraction.[45]

Since the development of OCT, interest in diagnosis of LMH has been renewed because high-resolution images can detect a lamellar macular defect that is not always visible clinically.[30,46] Data based on OCT proved that only 28% to 37% of LMHs are correctly diagnosed by biomicroscopy.[46,47] OCT enables clearly the differentiation between macular pseudoholes and LMHs.[46]

LMH has been described by OCT as a non-full-thickness defect of the macula with an irregular foveal contour and a dehiscence in the inner fovea, separation of the inner from the outer retinal layers, and absence of a full-thickness foveal defect with intact outer retinal layers at the base of the hole[47] (Figures 11 and 12).

Macular pseudohole was described on OCT picture as having a steep fovea contour and a normal or slightly increased central and paracentral retinal thickness[47] (Figures 13–15). Thus,

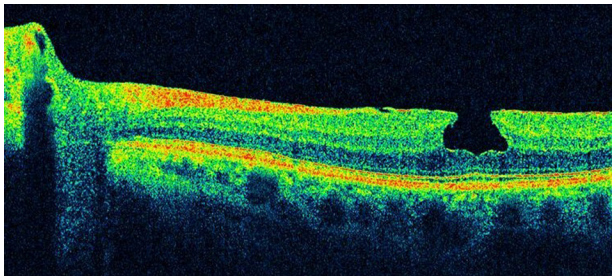

Figure 11 Spectral domain optical coherence tomography images of a 63-year-old male.
Notes: Macular pseudohole is shown, and an epiretinal membrane is evident. Observe that the foveal contour is beneath the line representing the outer plexiform layer. The photoreceptor layer is intact. Visual acuity was 20/40 and remained stable during 12 months of follow-up.

before the OCT era, many cases might have been misdiagnosed. In full-thickness macular holes, the percentage of coexisting epiretinal membranes confirmed with SD-OCT is about 13%.[48] Different authors have reported on epiretinal membranes coexisting with LMH in 62% to 73% of cases utilizing OCT.[49]

Witkin et al[46] reported that with ultrahigh-resolution OCT, epiretinal membranes are visible in 89% of LMH cases. Other observations demonstrate the presence of a hyper-reflective linear structure in all the cases of LMH.[50] LMH is generally regarded a clinically stable disorder. Theodossiadis et al[51] studied 41 patients with LMH and reported a mean decline of 6.4% in visual acuity (VA) after 37.1 months of observation.

Indications for surgical treatment of LMH remain controversial. A limited number of reports on vitrectomy results in

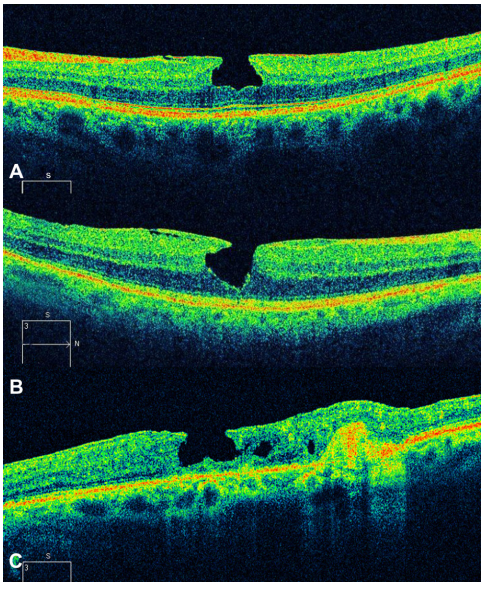

Figure 12 Spectral domain optical coherence tomography images of a 63-year-old male.
Notes: (**A**) Macular pseudohole. (**B**) Two examples of typical appearance of macular pseudohole with epiretinal membrane and a steeped foveal contour. (**C**) Macular pseudohole secondary to excessive laser scarring in parafoveal area.

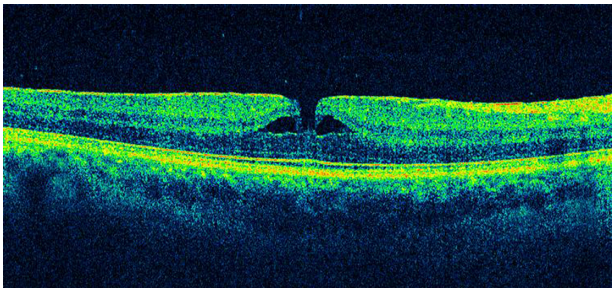

Figure 13 Pseudohole with lamellar defect.
Notes: Cystoid spaces exist around the pseudohole, but are separated from the pseudohole by tissue. Outer retinal tissue remains at the base of the fovea.

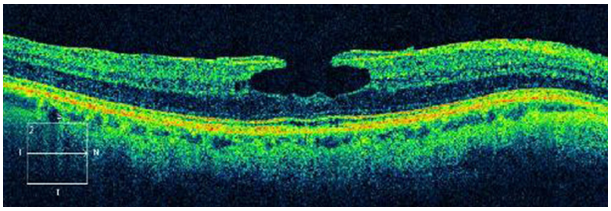

Figure 14 A 59-year-old male with lamellar macular hole.
Notes: A thicker epiretinal membrane was evident. Central foveal thickness remained stable throughout 12 months of follow-up. Outer nuclear layer is visible centrally.

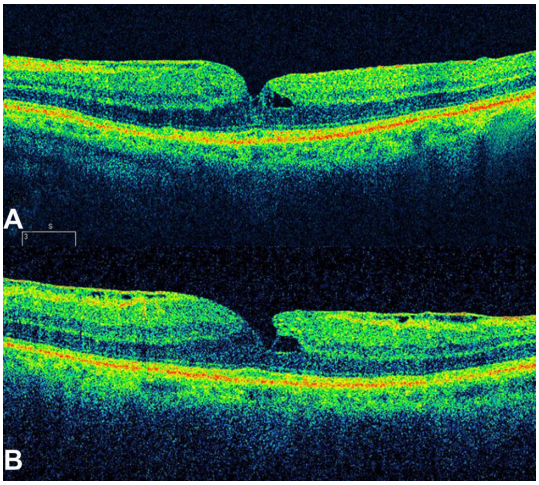

Figure 15 Macular pseudohole.
Notes: (**A**) Typical appearance of macular pseudohole with thin epiretinal membrane and a steeped foveal contour. (**B**) Three months after initial examination, cystoid spaces enlarged, with an irregular foveal contour and a schisis between the inner and outer retinal layers. An impending lamellar macular hole was created. No photoreceptor layer damage is present.

LMH patients have been published, and most studies reported favorable outcomes.[45,52–54] Recent reports on vitrectomy with removal of the ERM-ILM with or without gas injection demonstrated benefit both functionally and morphologically.[55,56] Bottoni et al[57] support previous indications[51] in planning treatment strategies; thus, vitrectomy could be indicated in LMHs showing a progressive thinning of foveal thickness and/or VA deterioration during the follow-up of the natural course of the

disease. Recently, Lee et al[58] indicated that a poor initial VA, the presence of a disrupted inner segment/outer segment (IS/OS) junction (Ellipsoid Zone), or a thin fovea on preoperative SD-OCT predicted poor vision outcome after LMH surgery. However, whether it is worthwhile to attempt surgical treatment for LMH remains a controversial issue.

Epiretinal membranes

Epiretinal membrane (ERM) is a disorder in which the vitreomacular interface induces a tangential tractional force on the retina, which can result in distortion of the macular architecture and development of vascular leakage with associated macular edema and vision loss.[11] Visual symptoms range from mild to severe and usually are manifested by blurred vision or metamorphopsia.

ERMs occur in 2.2% to 18.5%[59–62] of the population and can be either primary idiopathic, in which the incidence among elderly patients increases with age, or secondary to intraocular inflammatory conditions, retinal vascular disease, or occur after surgical intervention. Epiretinal membrane may also appear in otherwise healthy eyes as a result of incomplete vitreous detachment, and is typically characterized by the anatomic location of the ERM between the ILM and the vitreous body interface.[63]

Epiretinal membranes are caused by the migration of cells through small focal defects in the internal limiting membrane after posterior vitreous detachment, or by retinal breaks and detachments. These cells proliferate and create a thin veil of tissue at the retinal–vitreous interface. Purely glial cells are reported to occur in the earlier form of ERM, whereas a prominent fibrous, nonglial component has been reported in membranes causing traction.

Gass[64] proposed grading the severity of ERMs on the following clinical scale: Grade 0, translucent membranes unassociated with retinal distortion; Grade 1, membranes causing irregular wrinkling of the inner retina; and Grade 2, opaque membranes causing obscuration of the underlying vessels and marked full-thickness retinal distortion.

The early form of ERM, called cellophane macular reflex, is usually asymptomatic; therefore, most patients have normal or nearly normal vision with occasional metamorphopsia. However, the more severe form, known as macular pucker, can cause significant loss of visual acuity and visual symptoms such as distortion and metamorphopsia.[62] In very severe cases, macular edema and retinal detachment have been known to occur.

Mori et al[65] and Wilkins et al[66] classified ERM based on a scale secondary to OCT findings. OCT images of ERMs may be classified into two broad categories: globally adherent membranes or partially nonadherent membranes. Both types of ERMs are usually visible on OCT images as a taut hyperreflective line contiguous with or anterior to the inner retinal surface. The secondary effects of the membrane, such as loss of the normal foveal contour, variable irregularity of the inner retinal layers, and macular thickening, are used to establish the presence of the membrane.

OCT provides a means to evaluate the cross-sectional characteristics of epiretinal membrane, allowing a quantitative measurement of retinal thickness, membrane thickness, and the separation between the membrane and inner retina. Quantitative measurements of membrane thickness and reflectivity can be used to establish the degree of membrane opacity. The OCT tomogram can help to distinguish between membranes globally adherent to the retina, and epiretinal membranes separated from the inner retina.[66]

The appearance of such an ERM might be mimicked by a partially detached posterior vitreous surface. However, ERMs tend to be thicker and more reflective than the posterior vitreous. The reflection from an ERM may measure up to 60 μm in thickness; this is rarely observed with a partially detached posterior vitreous. Complete posterior vitreous detachment (PVD) is visible on the OCT image as a linear reflectivity suspended above the retinal surface (Figure 16). Epiretinal membranes are visible as a highly reflective layer on the inner retinal surface on OCT (Figures 17 and 18).

Characterization of the epiretinal membrane with OCT may help in preoperative planning for membrane peeling.[61] In cases with separation between the membrane and retina, the surgeon may be directed to these areas to initiate membrane dissection (Figures 19 and 20). When the membrane is globally attached to the inner retina, the surgeon may anticipate more difficulty in peeling the membrane (Figure 21). The surgeon may also proceed with particular caution when extensive intraretinal edema leaves a thin, friable inner retinal layer beneath the membrane. In most ophthalmology

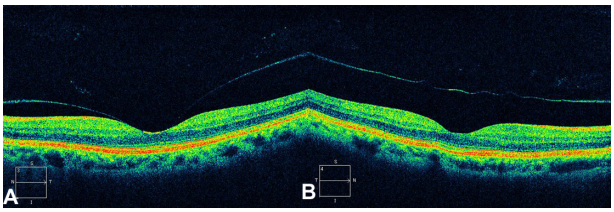

Figure 16 Posterior vitreous detachment.
Notes: (**A**) Partial posterior vitreous detachment is seen on this OCT image. (**B**) Complete posterior vitreous detachment is visible on the OCT image as a linear reflectivity suspended above the retinal surface.
Abbreviation: OCT, optical coherence tomography.

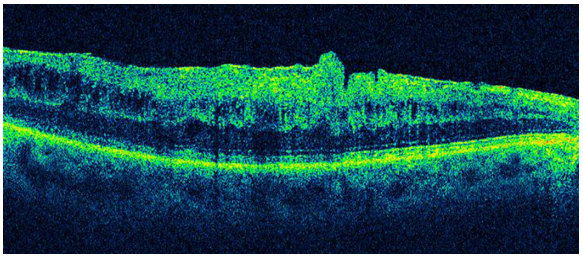

Figure 17 The epiretinal membrane is delineated as a highly reflective band and is globally attached to the retina.
Notes: There is a difference in reflectivity between the membrane and the underlying retina. The foveal depression was lost with intraretinal fluid accumulation.

centers, macular surgery for ERM removal is advocated if the best-corrected visual acuity falls below approximately 20/40, but there are no reports of objective indications for surgery, such as OCT findings.

Metamorphopsia induced by ERM may be related to the edematous areas of the inner nuclear layer detected with SD-OCT. The classification of ERM based on the inner nuclear layer thickness is a potentially useful indication for surgery.[60]

High-resolution OCT has several advantages for a detailed evaluation of vitreomacular traction (VMT) and ERM disease. The high-resolution representation of all intraretinal layers identifies the level and location of alterations in functionally relevant structures, such as the neurosensory architecture and the photoreceptor layer.[5,59]

Several factors, such as preoperative visual acuity,[67] duration of symptoms before surgery,[68] and the presence or absence of cystoid macular edema,[69] have been suggested as prognostic factors influencing the postoperative visual acuity. Investigators have suggested that the macular microstructure, such as macular thickness and appearance of the photoreceptor layer, may be associated with postoperative visual acuity.[70,71] The introduction of SD-OCT has improved the speed and sensitivity of the examination, allowing scanning at a higher resolution.

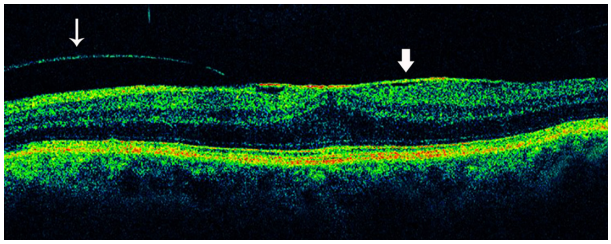

Figure 18 Partial posterior vitreous detachment and epiretinal membrane.
Notes: Partial posterior vitreous detachment (thin arrow) is seen as a hyper-reflective line above the retina and thinner than the epiretinal membrane (thick arrow). Epiretinal membranes are visible as a highly reflective layer on the inner retinal surface (thick arrow).

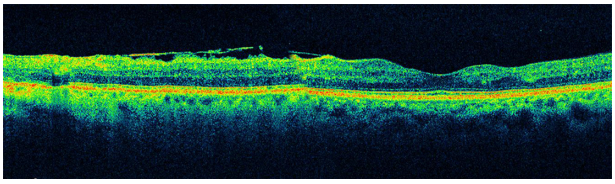

Figure 19 When the surgeon observes a separation between the epiretinal membrane and the retina, he or she may be directed to these areas to initiate membrane dissection.

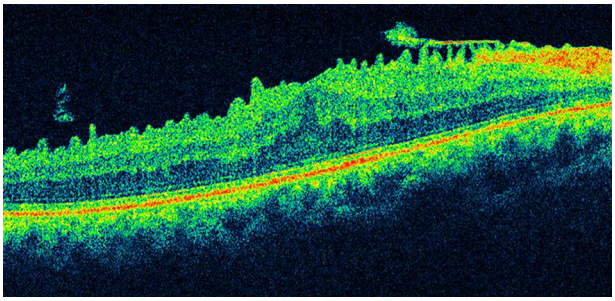

Figure 20 Another case of a partially adherent epiretinal membrane.
Note: There are numerous retinal folds on the internal layers of the retina secondary to partial detachment of the epiretinal membrane.

Therefore, postoperative OCT imaging can be used to document surgical response.

The photoreceptor layer can be imaged with SD-OCT as a hyper-reflective line showing the IS/OS junction or Ellipsoid Zone above the retinal pigment epithelium. An intact Ellipsoid Zone can be defined as a continuous hyper-reflective line, and the diagnosis of a disrupted IS/OS is made based on loss or irregularity of the hyper-reflective line corresponding to the Ellipsoid Zone. Existence of a correlation between photoreceptor IS/OS junction disruption and decreased postoperative visual acuity has been reported using time-domain OCT.[70,71] Macular edema resulting from the formation of ERM and some other artifacts may prevent a clear delineation of the IS/OS junction in time-domain OCT. However, SD-OCT allows more precise visualization of the intraretinal morphologic features, such as the external limiting membrane and the photoreceptor layer, thereby enabling clear measurements of the Ellipsoid Zone even in the presence of a thickened retina caused by the presence of an ERM.[72,73]

Vitreomacular traction syndrome

As the vitreous liquefies due to age, it detaches from the macula; this natural progression has been demonstrated using OCT in normal eyes.[74] However, in some people, an abnormally strong adhesion is present between the vitreous cortex and macula, and as the vitreous detaches

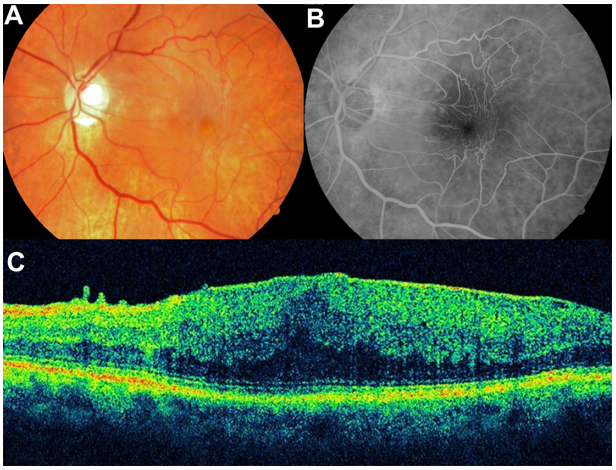

Figure 21 Epiretinal membrane.
Notes: (**A**) Color photograph of an epiretinal membrane. Vascular traction and loss of foveal reflex is observed. (**B**) Late fluorescein angiography demonstrates macular edema and vascular traction secondary to the epiretinal membrane. (**C**) Spectral domain OCT shows a continuous and adherent epiretinal membrane. Diverse and severe edematous changes in the inner nuclear layer, outer plexiform layer, and outer nuclear layer are seen on this OCT. When the membrane is globally attached to the inner retina, the surgeon may anticipate more difficulty in peeling the membrane.
Abbreviation: OCT, optical coherence tomography.

peripherally, it continues to pull on focal areas of the macula. This configuration appears identical to the vitreous attachment identified in idiopathic macular hole and cystoid macular edema or submacular fluid. Macular thickening caused by continued pathologic adherence of the vitreous to the retina in the setting of a peripheral vitreous detachment has been termed vitreomacular traction syndrome (VMTS).[53,75]

VMTS was first described in 1865 by Iwanoff [76] and refers to conditions in which retinal changes develop from incomplete posterior vitreous detachment with persistent vitreous adhesion to the macula, leading to morphologic distortion of the retinal surface as a result of the proliferation of myofibroblasts and the contractile element of the epiretinal membrane,[77] followed by functional changes such as metamorphopsia and visual deterioration. In a few of these eyes, the vitreous eventually separates from the macula on its own, leading to spontaneous resolution of vitreoretinal traction with normalization of the retinal contour and restoration of visual acuity. These changes have been documented with OCT.[78] However, in most eyes, vitreomacular traction persists and it can lead to progressive retinal edema, metamorphopsia, and/or visual deterioration. In these cases, vitrectomy may be an effective treatment option for patients with persistent and symptomatic vitreomacular traction diagnosed biomicroscopically.[79] Although the vitreous attachment to the macula usually appears broad on clinical exam, OCT typically shows an incomplete V-shaped posterior vitreous detachment temporally and nasally to the fovea, but with the fovea remaining attached (Figure 22). Early stages of PVD not detected biomicroscopically have been showed using OCT in normal subjects.[74] Therefore, in all cases with vitreoretinal interface abnormalities OCT is extremely useful for diagnosis and follow-up after treatment of these diseases. OCT images of the interface between the macula and vitreous are very well defined because of the difference in reflectivity of the relatively acellular vitreous and parallel-fiber orientation of the inner retina.[10] PVD is visible on the OCT image as a thin, moderately reflective band suspended above the macular surface when it separates from the retina (Figure 23).[80]

VMTS differs from idiopathic ERM in that the posterior hyaloid, rather than being totally detached from the posterior retina surface, remains attached to the perifoveal region. It is also frequently attached at the optic nerve and/or at multiple other points along or inside the vascular arcades. Sometimes the vitreous adherence can be difficult or impossible to identify directly on clinical exam. In VMTS, the PVD frequently is less reflective than ERMs and is associated with substantial foveal traction, intraretinal cystoid changes, cystoid macular edema, and foveal detachment. These changes result in central vision loss and metamorphopsia.

Other VMTS cases can have a PVD temporally to the fovea but no posterior vitreous detachment nasal to it. In these cases prominent CME may develop, which may result in a macular hole or macular atrophy.[81] On the other hand, persistent traction can lead to progressive retinal edema and thickening. Quantifying such changes with the OCT can be valuable in determining the need for and/or timing of surgical intervention. As with ERMs, OCT can provide useful information in counseling VMTS patients preoperatively with regards to visual potential. Eyes demonstrating massive

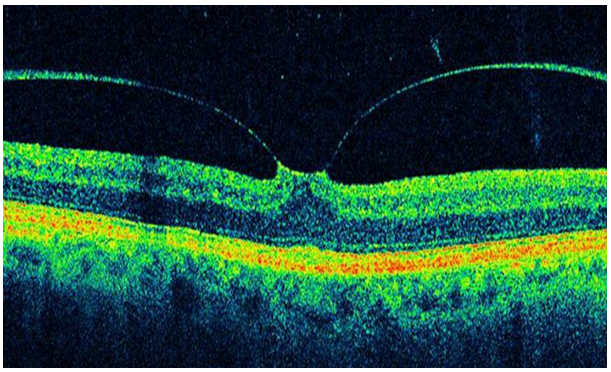

Figure 22 Optical coherence tomography typically shows an incomplete V-shaped posterior vitreous detachment temporally and nasally to the fovea that remains attached to the posterior vitreous.

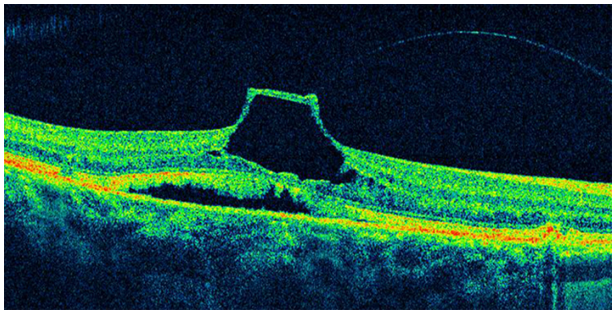

Figure 23 An incomplete posterior vitreous detachment with vitreomacular traction and tractional foveal detachment is observed on this optical coherence tomography image.

traction, distortion of retinal architecture, intraretinal edema, and foveal detachment may be anticipated to have a relatively poor ultimate outcome compared to eyes not exhibiting these features. After surgery, OCT can be used to evaluate the anatomic response (Figure 24). Case reports in the literature have documented improved retinal anatomy in association with increased visual acuity following vitrectomy surgery.[74,82]

High-resolution OCT has several advantages for a detailed evaluation of VMTS: raster scans provide a precise 2-D and 3-D image of the vitreomacular interface at each location. The high-resolution representation of all intraretinal layers identifies the level and location of alteration in functionally relevant structures, such as the neurosensory architecture and the photoreceptor layer.[4,59,83] Other advantages of SD-OCT are the improved axial resolution, higher scan speed, and the possibility of scanning the entire macular area at each location using the raster mode. These improvements enable better reproducibility of the same area of interest at each visit, and therefore enable superior results in a study aimed at evaluating distinct morphologic changes over time.

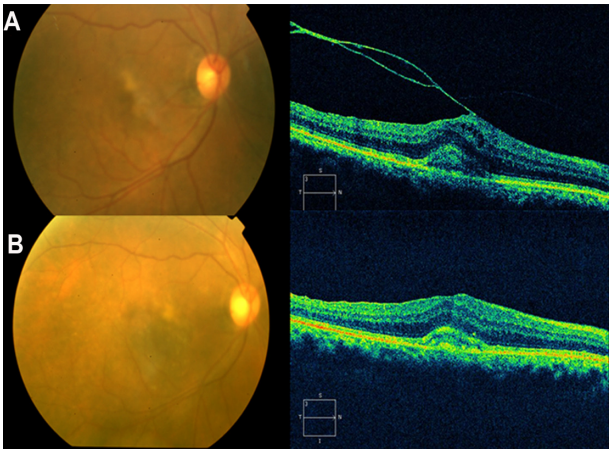

Figure 24 Pre- and postoperative OCT images.
Notes: (**A**) Preoperative OCT showed vitreomacular traction with attachment of the posterior hyaloid to the fovea. The tractional forces from the vitreous lead to the formation of macular edema, and accumulation of subfoveal pseudovitelliform yellowish material. (**B**) Postoperative OCT demonstrates relief of the vitreomacular traction after surgery, and a reduction of both macular edema and the subfoveal pseudovitelliform yellowish material.
Abbreviation: OCT, optical coherence tomography.

Recently, Sayegh et al[83] published a prospective analysis of the functional and morphologic parameters of retinal integrity over a 2-year follow-up in 30 patients undergoing vitreoretinal surgery for VMTS guided by high-resolution SD-OCT imaging. They observed that the best-corrected visual acuity did not correlate significantly with central retinal thickness or retinal volume; thus, a specific reduction of central retinal thickness and retinal volume has no significant effect on visual function. This result is consistent with the study of Haouchine et al[47] who measured central foveal thickness and reported no correlation with best-corrected visual acuity (BCVA). Furthermore, no correlation was found between the shape of the foveal contour, the presence of foveal cysts, or other morphologic parameters with BCVA.

The presence of the ERM induces folding and contraction of the retinal surface, and surgical release, including the internal limiting membrane, results in a rapid and impressive restoration of the retinal surface with disappearance of folds and reformation of the foveal contour. These morphologic changes seem to precede functional recovery. Visual rehabilitation proceeds over several months, reaching significance as late as 6 months after surgery. The integrity of the inner and, most importantly, the outer retinal layer follows a prolonged pattern of recovery as well. Recovery of inner/outer retinal layer proceeds slowly, reaching significance at 12 months, and correlated strongly with visual function. Therefore, reconstitution of neurosensory layers may be the most relevant parameter for visual improvement.

Vitreomacular traction and age-related macular degeneration

Vitreomacular traction alone is perhaps not able to induce age-related macular degeneration (AMD). However, it would seem sensible to consider vitreous changes when diagnosing and treating AMD patients because of the high coincidence of VMT and choroidal neovascularization and the often successful treatment of other diseases of the vitreoretinal interface by vitrectomy. The concept of the pathogenesis of AMD should therefore be extended to include the influence of the vitreous, especially where therapeutic concepts such as pharmacological vitreolysis and vitreous separation have been established as causative treatment of late forms of AMD.[84]

Krebs et al[85] described the presence of vitreomacular adhesions in 36% of eyes with exudative AMD, significantly

more frequently than in eyes with nonexudative AMD or control eyes. These results were confirmed by Robison et al,[86] who found vitreomacular adhesion (VMA) in 38% of eyes with exudative AMD, and by Lee et al,[87] who found VMA in 22.3% associated with neovascular AMD. These studies used primarily Stratus OCT examinations to verify VMA. Owing to the time-domain technology of Stratus OCT, differentiation between adhesion and traction was difficult, although traction was suspected in more than 50% of the cases. VMA but also signs of traction could clearly be identified in both SD-OCT machines, Spectralis and Cirrus OCT. Especially in the high-definition scans (five lines 6 mm in length in Cirrus OCT and one single line 8 mm in length in Spectralis OCT) the angulation of the posterior vitreous cortex was clearly visible. Furthermore, three-dimensional OCT (3D-OCT) shows splitting within the posterior vitreous cortex, in the area of vitreo papillary adhesion and traction from different directions. Three-dimensional OCT imaging was possible in most (83.3%) of the Cirrus SD-OCT cube scans, but only in 13.3% of Spectralis OCT volume scans of a sufficient scan density was possible.

Krebs et al[88] identified traction with adhesions in 73.3% of cases with exudative AMD and they showed that the location and the direction of the traction forces visualized by high-technology OCT and 3D-OCT correspond in 100% with the origin of the choroidal neovascularization.

Summary

In recent years, OCT has been established as a useful tool in the diagnosis and clinical evaluation of macular disease. OCT is now a standard of care in ophthalmology and is considered essential for the diagnosis and monitoring of many retinal diseases.

One of the major advances with OCT since its introduction has been the understanding of the pathophysiology of macular holes. Non-full-thickness macular holes have been revisited because high-resolution images can detect a lamellar macular defect that is not always visible clinically. It is reasonable to consider new therapeutic approaches with the identification of traction with adhesions in cases with exudative AMD by SD-OCT. OCT can be valuable in determining the need and/or timing of surgical intervention on vitreoretinal interface disorders.

Acknowledgments

This work was supported in part by the Arevalo-Coutinho Foundation for Research in Ophthalmology, Caracas, Venezuela. Presented in part at the LIX National Congress of Ophthalmology, Caracas, Venezuela, May 2011.

Disclosure

The authors declare no conflicts of interest in this work.

References

1. Fujimoto JG, Brezinski ME, Tearney GJ, et al. Optical biopsy and imaging using optical coherence tomography. *Nat Med*. 1995;1(9):970–972.
2. Brezinski ME, Tearney GJ, Bouma BE, et al. Optical coherence tomography for optical biopsy. Properties and demonstration of vascular pathology. *Circulation*. 1996;93(6):1206–1213.
3. Larsson J. Vitrectomy in vitreomacular traction syndrome evaluated by ocular coherence tomography (OCT) retinal mapping. *Acta Ophthalmol Scand*. 2004;82(6):691–694.
4. Ito Y, Terasaki H, Mori M, Kojima T, Suzuki T, Miyake Y. Three-dimensional optical coherence tomography of vitreomacular traction syndrome before and after vitrectomy. *Retina (Philadelphia, Pa)*. 2000;20(4):403–405.
5. Koizumi H, Spaide RF, Fisher YL, Freund KB, Klancnik JM, Yannuzzi LA. Three-dimensional evaluation of vitreomacular traction and epiretinal membrane using spectral-domain optical coherence tomography. *Am J Ophthalmol*. 2008;145(3):509–517.
6. Huang D, Swanson EA, Lin CP, et al. Optical coherence tomography. *Science*. 1991;254(5035):1178–1181.
7. Fercher AF, Roth E. Ophthalmic laser interferometry. *Proc SPIE*. 1986;658:48–51.
8. Fercher AF, Hitzenberger CK, Drexler W, Kamp G, Sattmann H. In vivo optical coherence tomography. *Am J Ophthalmol*. 1993;116(1):113–114.
9. Swanson EA, Izatt JA, Hee MR, et al. In vivo retinal imaging by optical coherence tomography. *Opt Lett*. 1993;18(21):1864–1866.
10. Hee MR, Izatt JA, Swanson EA, et al. Optical coherence tomography of the human retina. *Arch Ophthalmol*. 1995;113(3):325–332.
11. Voo I, Mavrofrides EC, Puliafito CA. Clinical applications of optical coherence tomography for the diagnosis and management of macular diseases. *Ophthalmol Clin North Am*. 2004;17(1):21–31.
12. Panozzo G, Gusson E, Parolini B, Mercanti A. Role of OCT in the diagnosis and follow up of diabetic macular edema. *Semin Ophthalmol*. 2003;18(2):74–81.
13. Massin P, Duguid G, Erginay A, Haouchine B, Gaudric A. Optical coherence tomography for evaluating diabetic macular edema before and after vitrectomy. *Am J Ophthalmol*. 2003;135(2):169–177.
14. Bouma B, Tearney GJ, Boppart SA, Hee MR, Brezinski ME, Fujimoto JG. High-resolution optical coherence tomographic imaging using a mode-locked Ti:Al(2)O(3) laser source. *Opt Lett*. 1995;20(13):1486–1488.
15. Drexler W, Morgner U, Kärtner FX, et al. In vivo ultrahigh-resolution optical coherence tomography. *Opt Lett*. 1999;24(17):1221–1223.
16. Drexler W, Morgner U, Ghanta RK, Kärtner FX, Schuman JS, Fujimoto JG. Ultrahigh-resolution ophthalmic optical coherence tomography. *Nat Med*. 2001;7(4):502–507.
17. Drexler W, Sattmann H, Hermann B, et al. Enhanced visualization of macular pathology with the use of ultrahigh-resolution optical coherence tomography. *Arch Ophthalmol*. 2003;121(5):695–706.
18. Ho AC, Guyer DR, Fine SL. Macular hole. *Surv Ophthalmol*. 1998;42(5):393–416.
19. Chew EY, Sperduto RD, Hiller R, et al. Clinical course of macular holes: the Eye Disease Case-Control Study. *Arch Ophthalmol*. 1999;117(2):242–246.
20. Chauhan DS, Antcliff RJ, Rai PA, Williamson TH, Marshall J. Papillofoveal traction in macular hole formation: the role of optical coherence tomography. *Arch Ophthalmol*. 2000;118(1):32–38.

21. Mori K, Abe T, Yoneya S. Dome-shaped detachment of premacular vitreous cortex in macular hole development. *Ophthalmic Surg Lasers*. 2000;31(3):203–209.
22. Gaudric A, Haouchine B, Massin P, Paques M, Blain P, Erginay A. Macular hole formation: new data provided by optical coherence tomography. *Arch Ophthalmol*. 1999;117(6):744–751.
23. Han IC, Jaffe GJ. Comparison of spectral- and time-domain optical coherence tomography for retinal thickness measurements in healthy and diseased eyes. *Am J Ophthalmol*. 2009;147(5):847–858, 858. e1.
24. Forooghian F, Cukras C, Meyerle CB, Chew EY, Wong WT. Evaluation of time domain and spectral domain optical coherence tomography in the measurement of diabetic macular edema. *Invest Ophthalmol Vis Sci*. 2008;49(10):4290–4296.
25. Hatef E, Khwaja A, Rentiya Z, et al. Comparison of time domain and spectral domain optical coherence tomography in measurement of macular thickness in macular edema secondary to diabetic retinopathy and retinal vein occlusion. *J Ophthalmol*. 2012;2012:354783.
26. Takahashi H, Kishi S. Tomographic features of a lamellar macular hole formation and a lamellar hole that progressed to a full-thickness macular hole. *Am J Ophthalmol*. 2000;130(5):677–679.
27. Gass JDM. Idiopathic senile macular holes: its early stages and pathogenesis. *Arch Ophthalmol*. 1988;106(5):629–639.
28. Johnson MW. Improvements in the understanding and treatment of macular hole. *Curr Opin Ophthalmol*. 2002;13(3):152–160.
29. Gass JDM. Reappraisal of biomicroscopic classification of stages of development of a macular hole. *Am J Ophthalmol* 1995; 119: 752–759.
30. Haouchine B, Massin P, Gaudric A. Foveal pseudocyst as the first step in macular hole formation: a prospective study by optical coherence tomography. *Ophthalmology*. 2001;108(1):15–22.
31. Avila MP, Jalkh AE, Murakami K, Trempe CL, Schepens CL. Biomicroscopic study of the vitreous in macular breaks. *Ophthalmology*.; 1983;90 (11):1277–1283.
32. Gass JD, Joondeph BC. Observations concerning patients with suspected impending macular holes. *Am J Ophthalmol*. 1990;109(6):638–646.
33. Gass JD. Age-dependent idiopathic macular foramen. Current concepts of the pathogenesis, diagnosis, and treatment. *Ophthalmology*. 1995; 92 (5): 617–625.
34. Lewis MI, Cohen SM, Smiddy WE, Gass JD. Bilaterality of idiopathic macular holes. *Graefes Arch Clin Exp Ophthalmol*. 1996;234(4): 241–245.
35. Spiritus A, Dralands L, Stalmans P, Stalmans I, Spileers W. OCT study of fellow eyes of macular holes. *Bull Soc Belge Ophtalmol*. 2000;275:81–84.
36. Kang SW, Ahn K, Ham DI. Types of macular hole closure and their clinical implications. *Br J Ophthalmol*. 2003;87(8):1015–1019.
37. Puliafito CA, Hee MR, Lin CP, et al. Imaging of macular diseases with optical coherence tomography. *Ophthalmology*. 1995;102(2):217–229.
38. Duker JS, Puliafito CA, Wilkins JR, et al. Imaging fellow eyes in patients diagnosed with idiopathic macular holes using optical coherence tomography (OCT). *Ophthalmology* 1995; 102: 118.
39. Benson SE, Schlottmann PG, Bunce C, Charteris DG. Comparison of macular hole size measured by optical coherence tomography, digital photography, and clinical examination. *Eye (Lond)*. 2008;22(1): 87–90.
40. Altaweel M, Ip M. Macular hole: improved understanding of pathogenesis, staging, and management based on optical coherence tomography. *Semin Ophthalmol*. 2003;18(2):58–66.
41. Tilanus MA, Cuypers MH, Bemelmans NA, Pinckers AJ, Deutman AF. Predictive value of pattern VEP, pattern ERG and hole size in macular hole surgery. *Graefes Arch Clin Exp Ophthalmol*. 1999;237(8): 629–635.
42. Ullrich S, Haritoglou C, Gass C, Schaumberger M, Ulbig MW, Kampik A. Macular hole size as a prognostic factor in macular hole surgery. *Br J Ophthalmol*. 2002;86(4):390–393.
43. Gass JD. Lamellar macular hole: a complication of cystoid macular edema after cataract extraction: a clinicopathologic case report. *Trans Am Ophthalmol Soc*. 1975;73:231–250.
44. Allen AW, Gass JD. Contraction of a perifoveal epiretinal membrane simulating a macular hole. *Am J Ophthalmol*. 1976;82(5):684–691.
45. Michalewska Z, Michalewski J, Odrobina D, et al. Surgical treatment of lamellar macular holes. *Graefes Arch Clin Exp Ophthalmol*. 2010;248(10):1395–1400.
46. Witkin AJ, Ko TH, Fujimoto JG, et al. Redefining lamellar holes and the vitreomacular interface: an ultrahigh-resolution optical coherence tomography study. *Ophthalmology*. 2006;113(3):388–397.
47. Haouchine B, Massin P, Tadayoni R, Erginay A, Gaudric A. Diagnosis of macular pseudoholes and lamellar macular holes by optical coherence tomography. *Am J Ophthalmol*. 2004;138(5):732–739.
48. Michalewska Z, Michalewski J, Nawrocki J. Can HRT be a useful tool in differentiating lamellar macular holes from full-thickness macular holes? *Ophthalmologe*. 2010;107(3):251–255. German.
49. Ophir A, Fatum S. Cystoid foveal oedema in symptomatic inner lamellar macular holes. *Eye (Lond)*. 2009;23(9):1781–1785.
50. Michalewska Z, Michalewski J, Odrobina D, Nawrocki J. Non-full-thickness macular holes reassessed with spectral domain optical coherence tomography. *Retina (Philadelphia, Pa)*. 2012;32(5):922–929.
51. Theodossiadis PG, Grigoropoulos VG, Emfietzoglou I, et al. Evolution of lamellar macular hole studied by optical coherence tomography. *Graefes Arch Clin Exp Ophthalmol*. 2009;247(1):13–20.
52. Hirakawa M, Uemura A, Nakano T, Sakamoto T. Pars plana vitrectomy with gas tamponade for lamellar macular holes. *Am J Ophthalmol*. 2005;140(6):1154–1155.
53. Witkin AJ, Castro LC, Reichel E, Rogers AH, Baumal CR, Duker JS. Anatomic and visual outcomes of vitrectomy for lamellar macular holes. *Ophthalmic Surg Lasers Imaging*. 2010;41(4):418–424.
54. Kokame GT, Tokuhara KG. Surgical management of inner lamellar macular hole. *Ophthalmic Surg Lasers Imaging*. 2007;38(1):61–63.
55. Garretson BR, Pollack JS, Ruby AJ, Drenser KA, Williams GA, Sarrafizadeh R. Vitrectomy for a symptomatic lamellar macular hole. *Ophthalmology*. 2008;115(5):884–886. e1.
56. Androudi S, Stangos A, Brazitikos PD. Lamellar macular holes: tomographic features and surgical outcome. *Am J Ophthalmol*. 2009;148(3):420–426.
57. Bottoni F, Deiro AP, Giani A, Orini C, Cigada M, Staurenghi G. The natural history of lamellar macular holes: a spectral domain optical coherence tomography study. *Graefes Arch Clin Exp Ophthalmol*. 2013;251(2):467–475.
58. Lee CS, Koh HJ, Lim HT, Lee KS, Lee SC. Prognostic factors in vitrectomy for lamellar macular hole assessed by spectral-domain optical coherence tomography. *Acta Ophthalmol*. 2012;90(8):e597–e602.
59. Legarreta JE, Gregori G, Knighton RW, Punjabi OS, Lalwani GA, Puliafito CA. Three-dimensional spectral-domain optical coherence tomography images of the retina in the presence of epiretinal membranes. *Am J Ophthalmol*. 2008;145(6):1023–1030.
60. Ng CH, Cheung N, Wang JJ, et al. Prevalence and risk factors for epiretinal membranes in a multi-ethnic United States population. *Ophthalmology*. 2011;118(4):694–699.
61. Klein R, Klein BE, Wang Q, Moss SE. The epidemiology of epiretinal membranes. *Trans Am Ophthalmol Soc*. 1994;92:403–425.
62. Mitchell P, Smith W, Chey T, Wang JJ, Chang A. Prevalence and associations of epiretinal membranes. The Blue Mountains Eye Study, Australia. *Ophthalmology*. 1997;104(6):1033–1040.
63. Koerner F, Garweg J. Vitrectomy for macular pucker and vitreomacular traction syndrome. *Doc Ophthalmol*. 1999;97(3–4):449–458.
64. Gass JDM. Stereoscopic atlas of macular diseases; Diagnosis and Treatment, 3rd ed. St Louis, CV Mosby, 1987. 716–717.
65. Mori K, Gehlbach PL, Sano A, Deguchi T, Yoneya S. Comparison of epiretinal membranes of differing pathogenesis using optical coherence tomography. *Retina (Philadelphia, Pa)*. 2004;24(1):57–62.
66. Wilkins JR, Puliafito CA, Hee MR, et al. Characterization of epiretinal membranes using optical coherence tomography. *Ophthalmology*. 1996;103(12):2142–2151.
67. Wong JG, Sachdev N, Beaumont PE, Chang AA. Visual outcomes following vitrectomy and peeling of epiretinal membrane. *Clin Experiment Ophthalmol*. 2005;33(4):373–378.

68. Rice TA, De Bustros S, Michels RG, Thompson JT, Debanne SM, Rowland DY. Prognostic factors in vitrectomy for epiretinal membranes of the macula. *Ophthalmology*. 1986;93(5):602–610.
69. Trese MT, Chandler DB, Machemer R. Macular pucker. I. Prognostic criteria. *Graefes Arch Clin Exp Ophthalmol*. 1983;221(1):12–15.
70. Suh MH, Seo JM, Park KH, et al. Associations between macular findings by optical coherence tomography and visual outcomes after epiretinal membrane removal. *Am J Ophthalmol*. 2009;147(3):473–480.
71. Mitamura Y, Hirano K, Baba T, Yamamoto S. Correlation of visual recovery with presence of photoreceptor inner/outer segment junction in optical coherence images after epiretinal membrane surgery. *Br J Ophthalmol*. 2009;93(2):171–175.
72. Michalewski J, Michalewska Z, Cisiecki S, Nawrocki J. Morphologically functional correlations of macular pathology connected with epiretinal membrane formation in spectral optical coherence tomography (SOCT). *Graefes Arch Clin Exp Ophthalmol*. 2007;245(11):1623–1631.
73. Oster SF, Mojana F, Brar M, Yuson RM, Cheng L, Freeman WR. Disruption of the photoreceptor inner segment/outer segment layer on spectral domain-optical coherence tomography is a predictor of poor visual acuity in patients with epiretinal membranes. *Retina (Philadelphia, Pa)*. 2010;30(5):713–718.
74. Uchino E, Uemura A, Ohba N. Initial stages of posterior vitreous detachment in healthy eyes of older persons evaluated by optical coherence tomography. *Arch Ophthalmol*. 2001;119(10):1475–1479.
75. Gass JDM. Macular dysfunction caused by vitreous and vitreoretinal interface abnormalities. In: Gass JDM. *Stereoscopic Atlas of Macular Diseases: Diagnosis and Treatment*. 4th ed. St Louis, MO: Mosby-Year Book, Inc; 1997: 903–914.
76. Iwanoff A. Beitrage zur normalen und pathologischen Anatomie des Auges. [Contributions to the normal and pathological anatomy of the eye]. *Arch Ophthalmol*. 1865;11:135–170.
77. Gandorfer A, Rohleder M, Kampik A. Epiretinal pathology of vitreomacular traction syndrome. *Br J Ophthalmol*. 2002;86(8):902–909.
78. Hikichi T, Yoshida A, Trempe CL. Course of vitreomacular traction syndrome. *Am J Ophthalmol*. 1995;119(1):55–61.
79. Smiddy WE, Michels RG, Glaser BM, deBustros S. Vitrectomy for macular traction caused by incomplete vitreous separation. *Arch Ophthalmol*. 1988;106(5):624–628.
80. Gallemore RP, Jumper JM, McCuen BW, Jaffe GJ, Postel EA, Toth CA. Diagnosis of vitreoretinal adhesions in macular disease with optical coherence tomography. *Retina (Philadelphia, Pa)*. 2000;20(2):115–120.
81. Yamada N, Kishi S. Tomographic features and surgical outcomes of vitreomacular traction syndrome. *Am J Ophthalmol*. 2005;139(1):112–117.
82. Munuera JM, García-Layana A, Maldonado MJ, Aliseda D, Moreno-Montañés J. Optical coherence tomography in successful surgery of vitreomacular traction syndrome. *Arch Ophthalmol*. 1998;116(10):1388–1389.
83. Sayegh RG, Georgopoulos M, Geitzenauer W, Simader C, Kiss C, Schmidt-Erfurth U. High-resolution optical coherence tomography after surgery for vitreomacular traction: a 2-year follow-up. *Ophthalmology*. 2010;117(10):2010–2017, 2017. e1.
84. Schulze S, Hoerle S, Mennel S, Kroll P. Vitreomacular traction and exudative age-related macular degeneration. *Acta Ophthalmol*. 2008;86(5):470–481.
85. Krebs I, Brannath W, Glittenberg C, Zeiler F, Sebag J, Binder S. Posterior vitreomacular adhesion: a potential risk factor for exudative age-related macular degeneration? *Am J Ophthalmol*. 2007;144(5):741–746.
86. Robison CD, Krebs I, Binder S, et al. Vitreomacular adhesion in active and end-stage age-related macular degeneration. *Am J Ophthalmol*. 2009;148(1):79–82. e2.
87. Lee SJ, Lee CS, Koh HJ. Posterior vitreomacular adhesion and risk of exudative age-related macular degeneration: paired eye study. *Am J Ophthalmol*. 2009;147(4):621–626. e1.
88. Krebs I, Glittenberg C, Zeiler F, Binder S. Spectral domain optical coherence tomography for higher precision in the evaluation of vitreoretinal adhesions in exudative age-related macular degeneration. *Br J Ophthalmol*. 2011;95(10):1415–1418.